EJN European Journal of Neuroscience

FENS Federation of European Neuroscience Societies

European Journal of Neuroscience, Vol. 39, pp. 919–933, 2014 doi:10.1111/ejn.12460

NEUROSYSTEMS

Spatially extended forward suppression in primate auditory cortex

Yi Zhou and Xiaoqin Wang

Laboratory of Auditory Neurophysiology, Department of Biomedical Engineering, Johns Hopkins University, School of Medicine, Baltimore, MD 21205, USA

Keywords: auditory cortex, forward masking, frequency tuning, spatial selectivity

Abstract

When auditory neurons are stimulated with a pair of sounds, the preceding sound can inhibit the neural responses to the succeeding sound. This phenomenon, referred to as 'forward suppression', has been linked to perceptual forward masking. Previous studies investigating forward suppression typically measured the interaction between masker and probe sounds using a fixed sound location. However, in natural environments, interacting sounds often come from different spatial locations. The present study investigated two questions regarding forward suppression in the primary auditory cortex and adjacent caudal field of awake marmoset monkeys. First, what is the relationship between the location of a masker and its effectiveness in inhibiting neural response to a probe? Second, does varying the location of a masker change the spectral profile of forward suppression? We found that a masker can inhibit a neuron's response to a probe located at a preferred location even when the masker is located at a non-preferred location of a neuron. This is especially so for neurons in the caudal field. Furthermore, we found that the strongest forward suppression is observed when a masker's frequency is close to the best frequency of a neuron, regardless of the location of the masker. These results reveal, for the first time, the stability of forward masking in cortical processing of multiple sounds presented from different locations. They suggest that forward suppression in the auditory cortex is spectrally specific and spatially broad with respect to the frequency and location of the masker, respectively.

Introduction

The temporal order in which stimuli appear is important to sensory experience. One notable example is forward masking in the auditory system, where a preceding masker sound can effectively conceal the following probe sound by as much as 50 dB (Oxenham, 2001). Traditionally, masking is thought to occur due to spread of excitation along the cochlea (Fletcher, 1940). The excitation is assumed to cause prolonged neural activity following masker offset (Plomp, 1964), impeding detection of the subsequent probe response. This view was later challenged by the phenomena of 'forward suppression' and 'two-tone suppression' found in the auditory nerve fibers. Studies show that probe response can be suppressed by a preceding tone at best frequency (BF; Harris & Dallos, 1979; Delgutte, 1990) or by a simultaneously presented off-BF tone (Sachs & Kiang, 1968). Further studies show that forward suppression is a predominant cause of altered probe responses observed in the midbrain (Nelson *et al.*, 2009) and auditory cortex (Calford & Semple, 1995; Brosch & Schreiner, 1997; Sutter *et al.*, 1999; Scholes *et al.*, 2011), suggesting alternative suppressive mechanisms that are generated in the central auditory system for the behavioral masking phenomenon.

In previous experiments, masking is typically tested with the co-located masker and probe stimuli delivered from a single loudspeaker in free-field or delivered directly to the ear. At the neural level, the interaction between masker and probe is usually analysed in terms of their frequency relationship. In natural environments, however, target and background/distracting sounds often come from multiple sound locations (e.g. in the 'cocktail party' condition). Very little is known about how changes in a masker's spatial location affect the neural responses to the frequency relationship between masker and probe. On the other hand, spatially dependent adaptation and forward suppression have been demonstrated in various auditory stages from the lateral superior olive (Park *et al.*, 2008) to the inferior colliculus (Litovsky & Yin, 1998; Dahmen *et al.*, 2010) and auditory cortex (Fitzpatrick *et al.*, 1999; Reale & Brugge, 2000; Mickey & Middlebrooks, 2005; Middlebrooks & Bremen, 2013). Because the primary focus of these previous studies was spatial hearing, noise and click sounds were often used. These broadband stimuli do not provide sufficient resolution for testing the frequency and spatial dependence of forward suppression. To our knowledge, no physiological experiments have systematically evaluated the effectiveness of forward suppression in both spatial and spectral domains.

In the present study, we designed a series of experiments to determine the spectral profile of forward suppression at varied masker locations. We carried out these experiments in both primary auditory cortex (A1) and adjacent caudal medial and caudal lateral field

Correspondence: Dr Y. Zhou, as above.
E-mail: yizhou@asu.edu

Received 21 June 2013, revised 22 October 2013, accepted 20 November 2013

(CM/CL) in awake marmoset monkeys. The experimental approach is similar to that used in our previous study (Zhou & Wang, 2012). In that study, broadband noise stimuli were used as the masker to test the level dependence of forward suppression. In the present study, pure-tone and narrow-band noise stimuli were used as the masker to test the spectral profiles of forward suppression. We found that moving the masker away from the center of the spatial receptive field (SRF) of a neuron reduced the response amplitude of a neuron to the masker. However, the location of the masker had little effect on the frequency dependence of forward suppression, which persisted even when the masker was delivered from a 'far' location, at which weak or no masker responses were observed.

Materials and methods

Animal preparation and electrophysiological procedures

A chronic recording preparation developed in our laboratory (Lu *et al.*, 2001) was used to record single-unit activity in the auditory cortex of awake common marmoset monkeys (*Callithrix jacchus*). All experimental procedures were approved by the Institutional Animal Care and Use Committee of the Johns Hopkins University following NIH guidelines. Detailed descriptions of procedures are provided in our previous study (Zhou & Wang, 2012).

Briefly, all subjects were trained to sit in a custom-designed primate chair. After 2–4 weeks of behavioral adaptation, a surgery was conducted to implant two headposts in the skull under sterile conditions with the animal deeply anesthetized by isoflurane (0.5–2.0%, mixed with 50% oxygen and 50% nitrous oxide). The headposts served to maintain a stable head orientation during electrophysiological recordings. To access the auditory cortex, small craniotomies (~1 mm in diameter) were made on the skull over the superior temporal gyrus to allow for the penetration of electrodes (tungsten electrodes, 2–5 MΩ impedance; A-M Systems, Carlsborg, WA, USA) via a hydraulic microdrive (Trent-Wells, Los Angeles, CA, USA). Single-unit activity was sorted online using a template-based spike-sorting program (MSD, Alpha Omega Engineering) and analysed using custom programs written in Matlab (Mathworks, Natick, MA, USA). The 25th, 50th and 75th percentiles of the signal-to-noise ratio (SNR) were 17, 21 and 25 dB, respectively, for neurons reported in this study. SNR was defined as $20\log_{10}(|V_{max}|/\sigma_n)$ in decibels, where V_{max} was the maximal deflection of a spike waveform and σ_n was the standard deviation (SD) of baseline activity. The median variability of the SNR of a neuron was 1.74 dB (SD) across stimulus sets tested.

Experimental setup and sound delivery

Experiments were conducted in a dimly lit, double-walled, sound-attenuated chamber (IAC-1024, Industrial Acoustics; 1.9 m × 2.2 m × 1.9 m) lined with ~3 inch acoustic absorption foam (Sonex, Illbruck). During experiments, the subject's head remained fixed and eye position was not controlled. An infrared camera was used to monitor the general behavior of the subject throughout a recording session. Fifteen loudspeakers (FT28D, Dome Tweeter, Fostex) were mounted on a semicircular frame covering the upper-level frontal field at a distance of ~80 cm from the head of a subject. Figure 1A shows the loudspeaker positions specified in azimuth (AZ) and elevation (EL) angles in a spherical coordinate system (see also fig. 1 in Zhou & Wang, 2012).

All stimuli were generated digitally at a sampling rate of 100 kHz, converted via a digital-to-analog interface (Tucker-Davis Technologies, TDT, DA4), attenuated (TDT, PA4), amplified (Crown Amplifier, D75A), and delivered to either one or two speakers (i.e. one- or two-source stimulation) using a 16-channel multiplexer (TDT, PM1). The loudspeaker impulse responses were obtained by 2^{14}-point Golay code stimulation (Zhou *et al.*, 1992) using a free-field microphone (B&K Type 4191; ½-in) placed on the top of the primate chair pointing towards the loudspeaker under test. Electrophysiological equipment such as the head-holder and

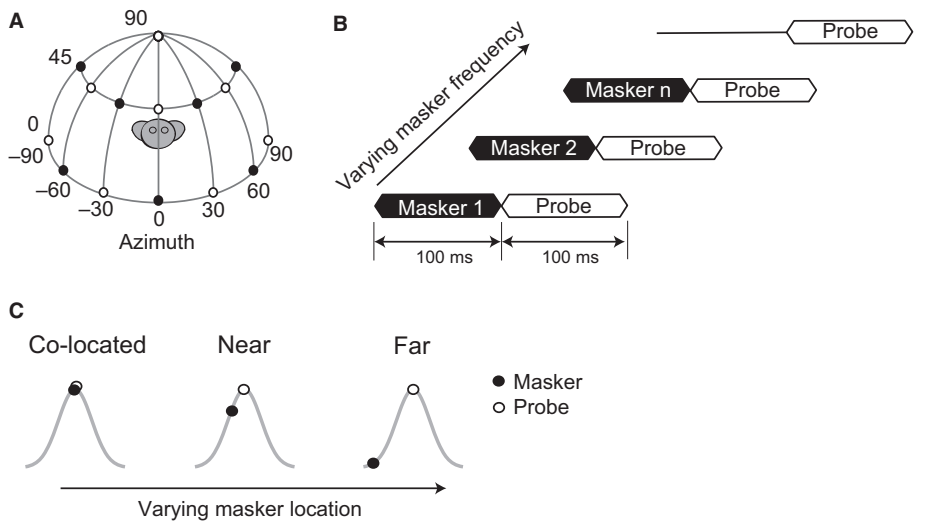

FIG. 1. Experimental setup for the modified 'forward-masking' paradigm. (A) Loudspeaker position in degrees. Seven loudspeakers were evenly positioned with 30° horizontal spacing (AZ ± 90°, ± 60°, ± 30°, 0°) at EL 0° and EL 45°; one loudspeaker was positioned directly above the head of a subject (EL 90°). The loudspeaker directly in front of the animal was at AZ 0° and EL 0°. Positive AZ angles reported in results corresponding to speakers ipsilateral to a recording site. (B) Masker-probe stimuli in the 'forward-masking' experiment. In the masker-probe trials, the masker frequencies were systematically varied as labeled from 1 to n, whereas the probe frequency remained fixed at BF and the probe was played immediately after masker offset. In the probe-alone trial, the masker was replaced by 100 ms silence. (C) Spatial arrangements of masker and probe locations. The solid line illustrates a hypothetical rate-location tuning curve of a neuron. The probe location is fixed at a preferred spatial location of a neuron, and the masker location is at 'co-located', 'near' or 'far' locations with an increasing distance to the probe.

electrode manipulator were removed during recording. We selected 16 loudspeakers that yielded relatively flat frequency responses out of 40 loudspeakers. For the chosen ones, the maximum deviation in power spectrum between responses of individual loudspeakers and their group average was within ± 6 dB/Hz in the frequency range of 2–32 kHz except for the top speaker, whose maximum deviation was about ± 12 dB/Hz due to reflections from the primate chair. Due to the finite frequency–response ranges of loudspeakers in our setup, acoustic stimuli were limited to the frequency range 2~32 kHz, with a few exceptions for testing frequency tuning of neurons whose maximal responses occurred below 2 kHz or above 32 kHz.

Characterizing basic response properties of A1 and CM/CL neurons

Single-unit responses were collected from A1 and the caudal field in four hemispheres of one male and two female adult marmoset monkeys between age 2 and 5 years. The tonotopic maps were reported in our previous study (Zhou & Wang, 2012). Because the medial to lateral division was not investigated in this study, we did not separate neurons further into CM and CL sectors. After a neuron was isolated, pure-tone and Gaussian noise stimuli (100 ms in duration with 5-ms cosine rise and fall times) were played iteratively to characterize its spatial, frequency and level selectivity. Frequency selectivity was typically examined using pure-tone stimuli (2~32 kHz in 10 steps/octave) played at moderate sound pressure levels (SPLs; 30–60 dB) from at least one driven speaker location. In general, BF was defined as the pure-tone frequency evoking the maximal firing rate of a neuron at the particular SPL tested (at least 10 dB above threshold) from one of the driven locations.

The threshold and minimum latency of a neuron were extracted from its rate-level responses to BF tones (−10 to 80 dB SPL in 10-dB increments). Threshold was defined as the lowest SPL evoking significant response (re. spontaneous discharge rate, R_{spont}, t-test, $P < 0.05$). For latency, we calculated the earliest time after stimulus onset where three consecutive 2-ms bins had discharge rates larger than 2 SDs above R_{spont} at each SPL. The minimum latency was defined as the smallest latency across the examined SPLs. This latency measurement is similar to previous studies in awake marmoset (Bendor & Wang, 2008) and macaque monkeys (Recanzone *et al.*, 2000).

Spatial sensitivity was evaluated using stimuli with varying bandwidths, including BF tone, BF-centered narrowband, and broadband frozen Gaussian noise (FIR filtered, flat spectrum between 2 and 32 kHz; at least 10 dB above the threshold). Noise samples were randomly chosen from neuron to neuron. Similar to those in our previous work (Zhou & Wang, 2012), the spatial sensitivity of a neuron was evaluated by its discharge rates. The rate-AZ tuning function was constructed based on the discharge rates of a neuron at various AZ speaker angles for EL 0° and 45°. For the purpose of visual inspection, we also constructed the 2D SRF using equal-area interpolation and extrapolation methods based on rate-location responses at 15 speaker locations. With θ in EL and ϕ in AZ, activity at a grid position (θ, ϕ) in an SRF was calculated as the weighted sum of responses over all speaker locations: $r(\theta, \phi) = \sum_{i=1}^{N} A_i R(\theta_i, \phi_i)$, where R (θ_i, ϕ_i) was the average firing rate to the ith speaker at the location (θ_i, ϕ_i), $N = 15$, and A_i was an exponential function $Ai = \exp(-\alpha^2/2\sigma^2)$ with $\sigma = 20°$, where α was the angular distance between (θ, ϕ) and (θ_i, ϕ_i). An SRF showed the peak-normalized r (θ, ϕ) with the abscissa for AZ and the ordinate for EL.

In the above analyses, the average discharge rate was calculated based on the number of spikes occurring 0–150 ms after the stimulus onset. Pure-tone and noise intensities were both expressed in terms of the peak-to-peak equivalent dB SPL. The reference amplitude was set by a 1-kHz tone calibrated at ~90 dB SPL (re. 20 μPa) with 0 dB peak attenuation. The spectrum level of noise was 40 dB/Hz at 0 dB peak attenuation. Ten repetitions were played for each stimulus with a minimum of 500 ms between stimuli.

Characterizing forward-suppression tuning curves of a neuron

Forward-suppression tuning curves were measured with a pair of lead-lag stimuli, where the lead was referred to as the masker and the lag as the probe. Figure 1B illustrates the stimulus arrangement in experiments. Similar to the previous 'forward masking' paradigm (e.g. Calford & Semple, 1995), the masker frequency was systematically varied and the probe was fixed at BF (pure-tone or BF-centered bandpass noise, if not driven by pure tones, with bandwidth no greater than 1.5 octave). This arrangement allowed simultaneous examination of: (1) the frequency tuning of the neuron's excitatory responses to the masker; and (2) the frequency tuning of forward suppression of the probe response caused by the introduction of the masker. In the masker-probe trials, the masker and probe each lasted 100 ms, and the probe was played immediately after the masker; no delay was imposed between masker offset (after 5 ms fall time) and probe onset (before 5 ms rise time). In the probe-alone trials, a period of silence of the same duration as the masker was inserted before the probe. The masker and probe were both played at moderate SPLs (at least 10 dB above the threshold), at which clear driven responses could be observed. The lower, median and upper quartiles of the masker SPL were 30, 40 and 50 dB SPL in A1, and 30, 40 and 60 dB SPL in CM/CL, respectively. The probe-alone and masker-probe trials were interleaved and presented in random order with an inter-trial interval of 500 ms.

We further extended the 'forward masking' paradigm by testing effects of the masker location on forward suppression. The spatial setup was similar to that used for testing 'spatial release from masking' in the auditory system (Lane & Delgutte, 2005). To achieve this, the 15 loudspeakers were divided into two channels (A and B) with an interleaved arrangement as shown in Fig. 1A. The interleaved arrangements of A and B allowed a broad coverage of the frontal field for both probe and masker stimuli to accommodate different spatial selectivity of cortical neurons.

In experiments, the probe was delivered from a loudspeaker in channel B (open circle, Fig. 1A). This location corresponded to one of the speaker locations that elicited maximal responses of a neuron. The masker was delivered from a loudspeaker in channel A (filled circle, Fig. 1A), which included speakers immediately adjacent to the probe location ('near' condition) and speakers far away from the probe location ('far' condition). In the 'near' condition, the AZ separation between masker and probe was either 0° if they were at different EL or 30° if they were at the same EL. In the 'far' condition, the AZ separation between masker and probe was at least 60°. Additionally, masker and probe were summed physically (TDT, SM3) and played from the same location ('co-located' condition). The exact positions of 'co-located', 'near' and 'far' varied from neuron to neuron, depending on the size and orientation of an SRF, and were chosen primarily based on a neuron's spatial selectivity to BF-tone and/or BF-centered bandpass noise.

As mentioned, two sets of rate–frequency curves were extracted from the forward-masking responses. They were: (1) tuning of masker responses, measured by the difference between the discharge

rate to the masker and spontaneous rate of the neuron, R(masker) – R(spont); and (2) the tuning of masker-evoked forward suppression, measured by the difference between the discharge rate to the probe with and without the preceding masker, R(probe|masker) – R(probe). Because these metrics were expressed relative to the spontaneous or probe-alone rate, positive and negative values were described as excitatory and inhibitory neural activity, respectively, in our analyses. For masker responses, spike counts were collected between 15 ms after masker onset and 15 ms after masker offset. For probe response, spike counts were collected between 15 ms after probe onset and 15 ms after probe offset. This 15-ms shift in data analysis was used to compensate the transmission delay from the loudspeaker to the ear (~2.5 ms) and to the auditory cortex (see 'latency analysis' in Results). It also helped prevent recruiting masker responses in the analysis of probe responses. For the population analysis, the rate–frequency curves measured at 'co-located', 'near' and 'far' locations of each neuron were normalized by the absolute peak value among them, thus preserving excitatory or inhibitory dynamic ranges of responses.

Additionally, we evaluated the temporal profiles of forward suppression by examining the post-stimulus time histograms (PSTHs) in response to masker and probe. The PSTHs were generated by counting spikes in fixed time bins as a function of time and then smoothing these time series using a Gaussian filter (which had a mean of zero and standard deviation of the bin-width) truncated at ± 3 SDs with unit energy. The data analysis used a 5-ms bin-width and the number of spikes per bin was averaged over 10 repetitions. Before averaging the results for a population of neurons, the spontaneous rate was subtracted from individual PSTHs to remove the baseline fluctuation. Then, for each neuron, the three PSTHs (for 'co-located', 'near' and 'far' conditions) were normalized by the maximal responses to obtain unified dynamic ranges of response across the population. Results with three masker frequencies (0.75BF, BF, 1.25BF) were shown.

Results

Basic response properties of neurons in A1 and CM/CL

Single-unit data were collected from four hemispheres in three adult marmosets. Figure 2A shows the locations of recording sites and BF distribution in the left hemisphere of one subject. In our studies, the majority of neurons were recorded from areas within a distance of 3 mm to the lateral sulcus on the superior temporal gyrus through lateral penetrations of microelectrodes. The tonotopy reversal was used to distinguish A1 from CM/CL (Merzenich & Brugge, 1973; Aitkin *et al.*, 1986). The tonotopic mapping of other hemispheres is reported in our previous study (Zhou & Wang, 2012). The analyses

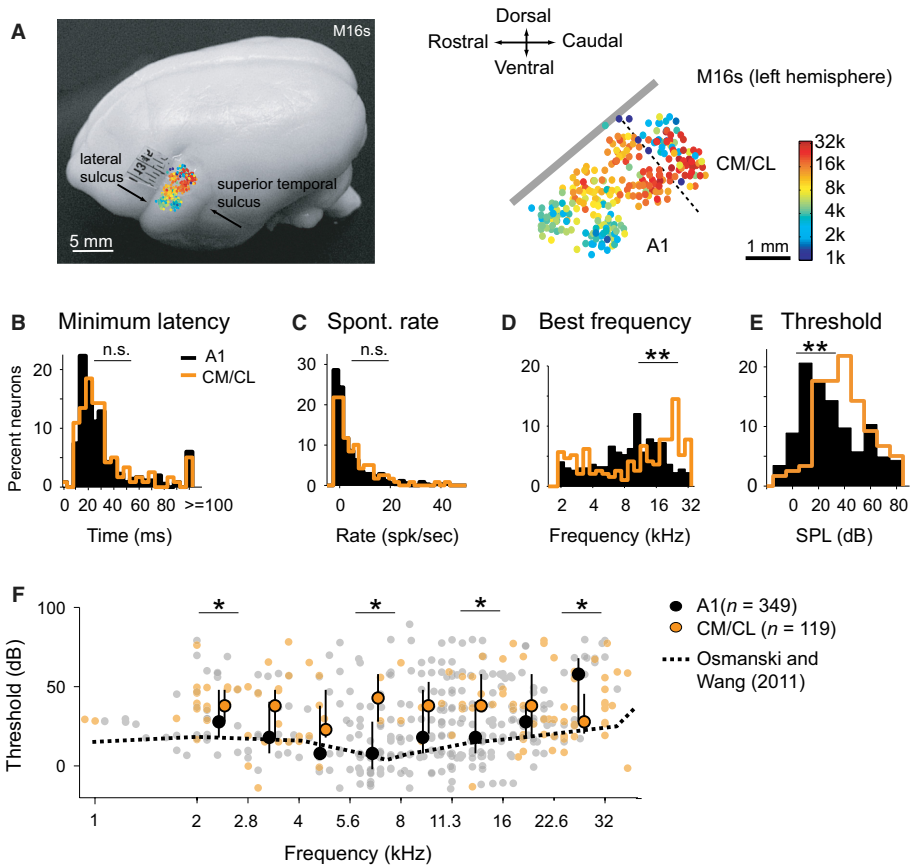

FIG. 2. Comparison of basic response properties between primary auditory cortex (A1) and caudal medial (CM)/caudal lateral (CL) neurons. (A) The lateral view of the left hemisphere of one subject. The colored dots indicate the BFs of individual neurons collected through lateral penetrations made on the surface of the superior temporal gyrus. The detailed organization of the tonotopy is shown on the right. Gray line, lateral sulcus. Dashed line, the tentative separation between area A1 and CM/CL. (B–E) Comparison of minimum latency, spontaneous rate, BF, threshold distributions in areas A1 and CM/CL. (F) BF-tone thresholds of A1 and CM/CL neurons. For statistical analyses, neurons were divided into seven non-overlapping BF groups from 2 to 32 kHz (half-octave width). The filled circles indicate the median, and vertical bars indicate 25th–75th percentile of a data distribution. The bin-width was 0.2 octaves for BF, 10 dB for threshold, 5 ms for latency and 2 spk/s for spontaneous rate. *P < 0.05, **P < 0.001, n.s., not significant. Spont, spontaneous.

shown here compare the response latency, frequency preference and response threshold of 349 A1 units and 119 CM/CL units we collected.

Distributions of minimum latency (Fig. 2B) and spontaneous discharge rate (Fig. 2C) in A1 were similar to those found in CM/CL ($P > 0.05$, Wilcoxon rank-sum test). However, the overall frequency preferences of neurons were different between the two cortical fields (Fig. 2D). In A1, the BF distribution shows a peak in the intermediate frequency range (6~16 kHz). In contrast, a bimodal BF distribution was observed in CM/CL and the intermediate frequency range was under-represented. Marked differences were also found in the thresholds of BF-tone responses between A1 and CM/CL (Fig. 2E). On average, CM/CL neurons had higher thresholds than A1 neurons ($P < 10^{-5}$, Wilcoxon rank-sum test). Further analyses revealed that the minimum latency and spontaneous rate in A1 and CM/CL showed no significant correlations with BF (A1: $r < 0.04$, $P > 0.37$; CM/CL: $r < 0.1$, $P > 0.26$; Spearman's rank correlation). However, significant correlation between threshold and BF was found in A1 ($r = 0.19$, $P < 0.001$; Spearman's rank correlation). As shown in Fig. 2F, the thresholds of A1 neurons (median, black circles) were lowest at the mid-frequency range (4–8 kHz), similar to the behavioral pure-tone thresholds of marmosets (dashed line; Osmanski & Wang, 2011). This trend was not found in the thresholds of CM/CL neurons ($r = -0.03$, $P = 0.72$; Spearman's rank correlation), which exhibited relatively constant thresholds across frequencies (median, orange circles). In comparison, A1 neurons exhibited lower BF-tone thresholds than CM/CL neurons below 16 kHz, and CM/CL neurons exhibited similar or even lower thresholds than A1 neurons above 16 kHz. Table 1 summarizes the statistical analyses of these results.

Examples of forward suppression responses

We used a pair of masker-probe stimuli to examine the spectral selectivity of forward suppression in A1 and CM/CL of the marmoset auditory cortex. In the experiments, the masker and probe were presented sequentially with no delay between masker offset and probe onset (Fig. 1B). The probe was always played from a speaker location at or near the center of a neuron's SRF. The masker was played from one of three selected locations, either co-located with or away from the probe location (denoted as 'co-located', 'near' and 'far' conditions; Fig. 1C), similar to those used in the 'spatial release from masking' studies (Lane & Delgutte, 2005). Using this setup, we investigated the effect of masker location on forward masking responses of cortical neurons.

Figure 3 shows the results of two example A1 neurons. Their spatial selectivity was evaluated by rate-AZ tuning curves collected at EL 0° and 45°. For the purpose of illustration, we then derived smoothed 2D SRFs shown as heat maps. The first neuron responded to BF-tone stimuli at all frontal field locations. No clear AZ preference was observed, and responses at EL 45° were stronger than those at EL 0° (Fig. 3A). Figure 3B shows this neuron's responses to sequentially presented masker-probe stimuli at the three tested masker locations. For this neuron, the probe was delivered from an ipsilateral location, and the masker was placed at either the ipsilateral or contralateral side of the SRF (top panel, Fig. 3B). As seen in the dot-raster plots, the masker evoked strong excitation around BF at 4 kHz (0–100 ms) followed by weak suppression of the probe response (100–200 ms). This excitation–suppression pattern is consistently observed for all three masker locations.

We further quantified: (1) the frequency tuning of masker-evoked excitation by the difference between the discharge rate during masker and spontaneous discharge rate; and (2) the tuning of masker-evoked forward suppression by the difference between the discharge rate during probe with the preceding masker and the discharge rate when the probe was played alone. We compared the measurements for each of three masker locations (bottom panel, Fig. 3B). On these plots, the tunings of masker-evoked excitation and forward suppression are shown by red and black curves, respectively. It can be seen that the frequency tuning of forward suppression reached the maximum (i.e. mostly negative on black curves) around BF (dashed lines). For this neuron, frequency characteristics of forward suppression were not affected by the masker location. This means that probe responses could be suppressed by the same masker sound even when it was moved further away from the probe.

Intuitively, the above results might not be surprising in that neurons with a broad SRF, such as this one, are expected to perform a location-independent frequency analysis in the auditory cortex (Middlebrooks & Pettigrew, 1981). Yet, we found that location-independent forward suppression was not limited to neurons with broad SRFs. One such example is shown in Fig. 3C and D. This neuron had a restricted contralateral spatial preference for BF-centered bandpass noise (8 kHz, 1.25 octave). Similar to the results shown in Fig. 3B, forward suppression was observed when the masker and probe were both played from locations within the excitatory region of the SRF (first and second columns, Fig. 3D). However, when the masker was moved to an ipsilateral 'far' location outside the neuron's SRF, it evoked equally strong forward suppression around BF (third column, Fig. 3D). Note that the suppression observed had similar magnitude and frequency tuning for the three tested masker locations (black curves, Fig. 3D), whereas the excitation did not (red curves, Fig. 3D). It is worth emphasizing that the example in Fig. 3D shows that a masker presented from a 'far' location, to which the neuron was normally non-responsive, could actively suppress a neuron's responses to a probe presented from its preferred spatial location.

TABLE 1. Basic response properties of neurons in A1 and CM/CL

	BF (kHz)		Threshold (dB)		Minimum latency (ms)		Spontaneous rate (spk/s)	
Area (# neurons)	A1 ($N = 499$)	CM/CL ($N = 193$)	A1 ($N = 349$)	CM/CL ($N = 119$)	A1 ($N = 349$)	CM/CL ($N = 119$)	A1 ($N = 349$)	CM/Cl ($N = 119$)
Median	10.2	13.8	20	40	24	24	2.8	4
Rank-sum	$P < 0.001$		$P < 10^{-5}$		$P = 0.57$		$P = 0.06$	
Two-sample Kolmogorov–Smirnov	$P < 10^{-7}$		$P < 0.001$		$P = 0.34$		$P = 0.26$	

BF, best frequency.

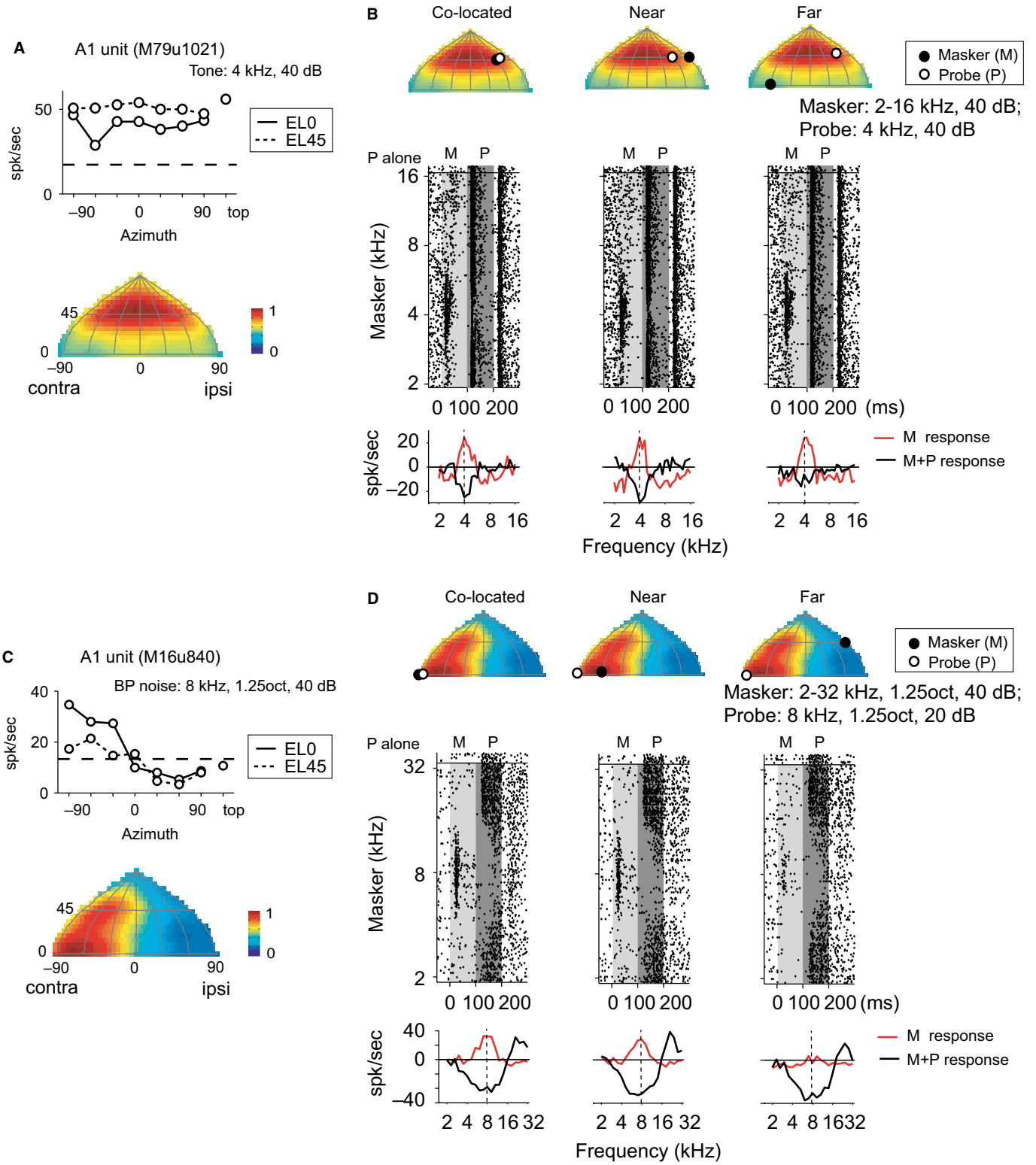

FIG. 3. Example of forward suppression in response of two A1 neurons. (A) The rate-azimuth (AZ) tuning function and 2D SRF of an primary auditory cortex (A1) neuron in response to BF tone. The dashed line indicates the spontaneous rate. (B) Responses of the neuron shown in (A) to a pair of masker-probe stimuli. The top row shows the locations of masker and probe used for 'co-located', 'near' and 'far' conditions, respectively. The middle row shows the dot-raster plots of responses for each spatial arrangement. Light and dark gray mark the durations of masker and probe, respectively. For comparison, the probe-alone responses are given on the top of each raster plot. The bottom row shows rate–frequency tunings of excitation (red) and forward suppression (black) for each spatial arrangement. All tuning curves are plotted as a function of masker frequency (see text for the methods of calculation). Masker and probe were both pure-tone stimuli, whose parameters were given on the plot. The dashed line indicates BF. (C and D) Spatial tuning and forward-masking responses of another A1 neuron. The data are presented in the same format as those in (A) and (B). Masker and probe were both bandpass (BP) noise stimuli. Contra, contralateral; EL, elevation; ipsi, ipsilateral; M, masker; P, probe. [Color version of figure available online].

Suppression of the probe response by maskers located at 'far' locations at specific masker frequencies was observed in the responses of many neurons in A1 and CM/CL. Two further examples showing this phenomenon are shown in Fig. 4; one from CM/CL and the other from A1. The CM/CL neuron had a spatial preference restricted to midline-ipsilateral locations (Fig. 4A). The probe was presented from a preferred location in the ipsilateral field (−30° in AZ) slightly off the peak of the SRF. The neuron responded strongly to the masker around 35 kHz at the 'co-located' and 'near' locations, but not the 'far' location outside its SRF (Fig. 4B). Regardless, the maskers with frequencies between 16 and 40 kHz caused complete suppression of probe responses at all three masker locations.

The SRF of the A1 neuron shown in Fig. 4C and D was restricted to contralateral locations (Fig. 4C). Unlike previous examples, this neuron showed an unusual mismatch between excitation and suppression center frequencies. While the maximal excitation was centered around 3 kHz, the maximal suppression occurred at higher masker frequencies between 4 and 6 kHz where the masker did not evoke excitation by itself (Fig. 4D). As shown in the following population analysis, this type of frequency mismatch was not typical in A1 and CM/CL.

Frequency dependence of forward suppression does not change with masker location

We examined a total of 101 single units using the forward masking protocol. Neural activities of 12 units were lost before the test was complete, which required sampling from at least three masker locations. For those completed, six units showed no driven responses and another six units showed no significant forward suppression to the test stimuli. They were excluded from the population analysis. The remaining 77 units (56 in A1 and 21 in CM/CL) all showed statistically significant excitatory responses and forward suppression from at least one tested spatial location (*t*-test, $P < 0.05$).

Figure 5 plots the results for A1 neurons. Figure 5A shows the frequency ranges of excitatory responses in 56 A1 units, arranged by unit's BF in ascending order from bottom to top. Shaded gray shows the frequency range tested for each neuron. Black dots show the masker frequencies at which a neuron's driven rate, in response to masker alone, exceeds 50% of its maximal rate within its SRF ('co-located' or 'near' locations). In general, moving the masker from 'co-located' to 'near' locations did not markedly change the frequency range of excitation. Moving the masker further away to 'far' locations reduced and even eliminated the excitatory responses in many neurons. This result is expected because most A1 neurons in marmoset auditory cortex have restricted SRFs in the frontal hemifield (Zhou & Wang, 2012). Figure 5B shows the population averages of the data shown in Fig. 5A, aligned by the BF of each unit. Although the response magnitude was reduced by 23.8% around BF from 'co-located' to 'far' locations, the frequency tuning and range of excitation were apparently not affected by stimulus location.

Figure 5C shows the frequency range of forward suppression measured from the same population of neurons arranged in the same order as that in Fig. 5A. Black dots indicate masker frequencies that caused more than 50% of the maximal forward suppression. Shaded gray shows the frequency range tested for each neuron. Note that many A1 neurons still exhibited forward suppression at 'far' locations (Fig. 5C, third column). The population averages in Fig. 5D show that the maximal suppression centered at BF. The reduction of the strength of forward suppression from 'co-located' to 'far' locations was 13% (Fig. 5D). Although this number is less than the reduction of the strength of excitation (Fig. 5B), pair-wise comparisons of results of individual neurons did not show significant differences between the changes in peak excitation and those in peak suppression when the masked moved from 'co-located' to 'far' locations (paired-sample *t*-test, $P = 0.137$).

The results in Fig. 5B and D also indicate that on average tuning of excitation and suppression both peaked around BF. Yet as shown in example responses (e.g. Fig. 4C and D), this is not always the case. To assess the degree of alignment between the absolute peaks of two sets of tuning curves, the BFs of suppression are plotted against the BFs of excitation for each unit (Fig. 5E). These two BF measurements were highly correlated at all three masker locations (linear regression, $P < 10^{-9}$). Among 56 A1 neurons collected, a majority of them had BFs for excitation and suppression that differed less than half an octave (41/56 for 'co-located', 41/56 for 'near' and 39/56 for 'far' locations).

Similar response properties were observed in CM/CL (Fig. 6). Note that while responses of many neurons to masker alone were greatly reduced when the masker was moved to a 'far' location (Fig. 6A and B), forward suppression persisted and the averaged tuning did not deviate substantially from those at 'co-located' and 'near' conditions (Fig. 6C and D). Analyses of results of individual neurons report significant differences between changes in peak excitation and those in peak suppression when the masker moved from 'co-located' to 'far' locations (paired-sample *t*-test, $P = 0.002$). It appears that masker location influenced the strength of forward suppression to a lesser degree in CM/CL than in A1. While on average masker responses almost reached the minimal strength at 'far' locations, the reduction of the strength of forward suppression from 'co-located' to 'far' locations was merely 0.6% at BF in CM/CL. Unlike those in A1 (Fig. 5E), the BFs of excitation and suppression appear to be less tightly distributed along the diagonal line in CM/CL (Fig. 6E). In comparison with A1, the percentage of neurons that had BFs for excitation and suppression differing less than half an octave was lower in CM/CL (14/21 for 'co-located', 13/21 for 'near' and 8/21 for 'far' locations). Further linear regression analyses indicated that masker and probe spectral sensitivity were significantly correlated at 'co-located' ($P = 0.006$) and 'near' ($P = 0.021$) conditions, but not at the 'far' condition ($P = 0.329$). This occurred in part because the BF estimate became unreliable due to weak excitatory responses at the 'far' condition.

Further analyses were performed to quantify the extent of changes in the shape of frequency tuning for individual neurons as a result of changing masker location. The analysis compared tuning curves measured from the 'co-located' condition with those measured from either the 'near' or 'far' condition using the Pearson correlation coefficient (CC). CC_{masker} describes the similarity in tuning of masker responses, and CC_{probe} describes the similarity in tuning of suppression of the probe responses. A total of 112 pair-wise correlations (56 × 2 pairs, 'co-located' vs. 'near' and 'co-located' vs. 'far') were analysed for A1 neurons, and 42 pair-wise correlations (21 × 2 pairs) were analysed for CM/CL neurons. The tuning functions of many neurons were preserved despite changes in masker location. For masker responses, the lower, median and upper quartiles of CC_{masker} were, respectively, 0.58, 0.78 and 0.89 in A1, and 0.33, 0.64 and 0.84 in CM/CL. For forward suppression, the lower, median and upper quartiles of CC_{probe} were 0.45, 0.65 and 0.73 in A1, and 0.34, 0.57 and 0.72 in CM/CL.

For a more detailed inspection, we then plotted these correlation values against the absolute AZ difference (ΔAZ) between masker and probe. In A1 (Fig. 7A), we found no significant effects of AZ

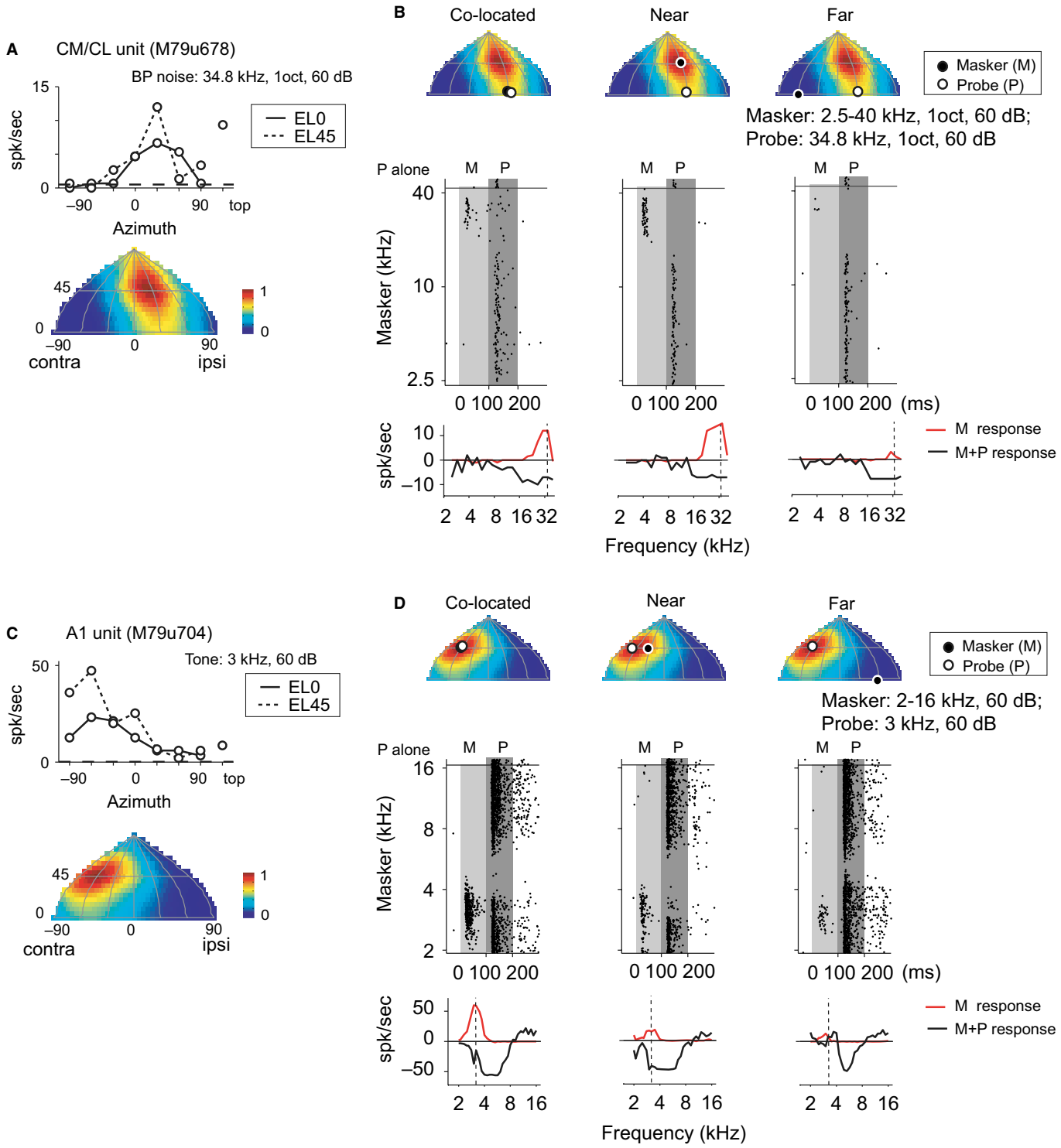

FIG. 4. Two examples showing that the masking effect was independent of the strength of masker response. (A and C) Spatial tuning and (B and D) forward-suppression responses of the two neurons. The data are presented in the same format as those in Fig. 3. The neuron in (B) showed complete suppression of the probe response when the masker was presented from a location outside the neuron's SRF (i.e. 'far' condition). The neuron in (D) showed complete suppression of the probe response caused by off-BF maskers with no preceding masker responses at either of three locations. A1, primary auditory cortex; CL, caudal lateral; CM, caudal medial; EL, elevation.

separation on the tuning curve similarity for masker responses (CC_{masker}; $r = -0.17$, $P = 0.07$) and forward suppression (CC_{probe}; $r = -0.18$, $P = 0.06$); Spearman's rank correlation. Many neurons showed high correlation values (> 0.5) even when the masker and probe were separated by 90 ° in AZ. In CM/CL (Fig. 7B), tuning curves became less similar in shape when the masker was moved further away from the probe as shown by decreased correlation values with AZ separation. This trend was more significant for tuning of masker responses (CC_{masker}: $r = -0.53$, $P = 0.0003$) than tuning of forward suppression (CC_{probe}: $r = -0.31$, $P = 0.04$). This noted

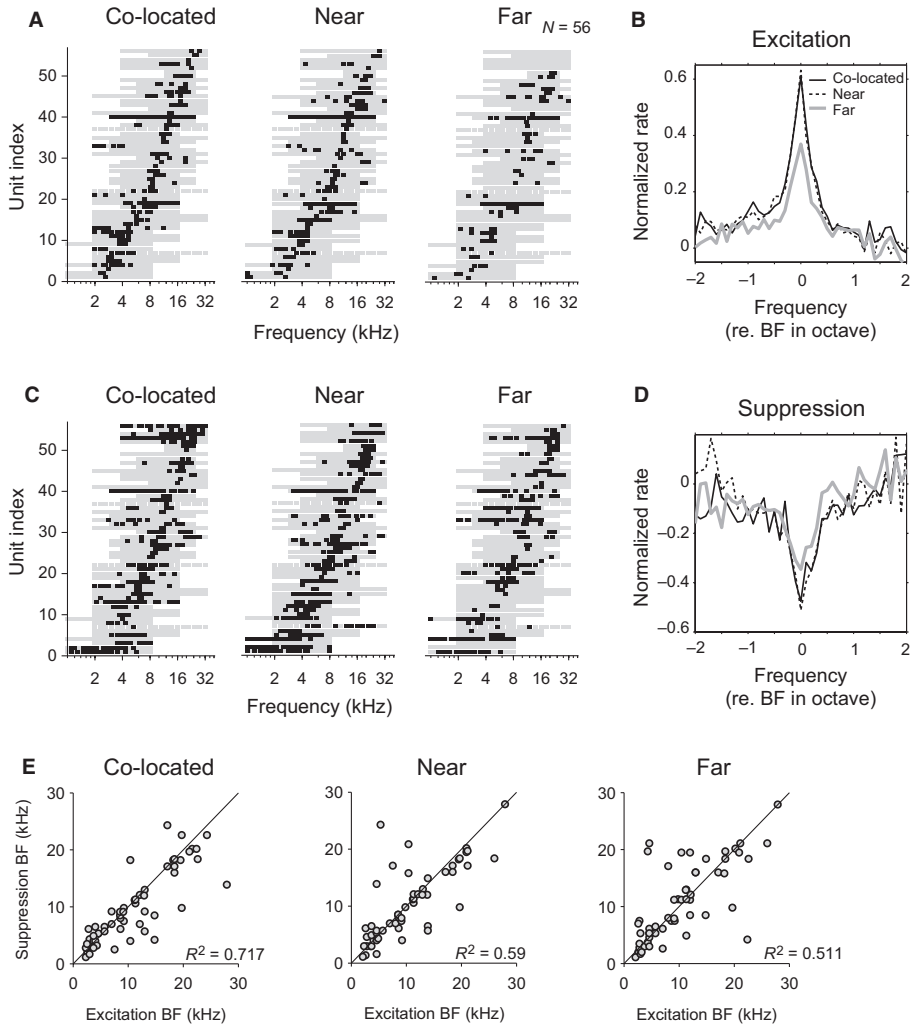

FIG. 5. Population analysis of the spectral extent of forward suppression in A1. (A) Distribution of the excitatory masker frequencies. At these frequencies, the firing rate of a neuron was more than 50% of its peak rate observed across all three masker locations. (B) Population average of normalized rate–frequency tuning of masker-evoked excitation. (C) Distribution of the inhibitory masker frequencies. At these frequencies, the reduction of the probe response exceeded 50% of the maximal reduction observed across all three masker locations. (D) Population average of normalized rate–frequency tuning of masker-evoked suppression. To obtain normalized responses of a neuron, its rate–frequency curve at a location was divided by the maximal absolute response rate (maximal excitation or maximal reduction) among the three tuning curves collected at 'co-located', 'near' and 'far' locations. (E) Pair-wise comparisons of the alignment between frequencies of masker associated with maximal masker responses [best frequencies (BFs) of excitation] and maximal forward suppression (BFs of suppression). Bin-width, 0.2 octaves.

dependence in masker responses was caused by reductions of discharge rates of neurons at 'far' locations (CC_{masker}: $P < 10^{-5}$; CC_{probe}: $P < 0.01$). Despite the trend observed, the weak responses did not yield sufficient estimation power for correlation analyses as shown above. None of the low CC values (CC < 0.35) in CM/CL results was statistically significant.

Finally, testing for EL was limited to 0° or 45°. Correlation values CC_{masker} and CC_{probe} showed no significant correlations with masker EL ($P > 0.1$; Spearman's rank correlation).

Temporal profile of forward suppression does not change with masker location

To characterize the temporal profiles of forward suppression, we analysed the population-averaged PSTHs for masker-probe responses. Figure 8 shows the population PSTHs at three representative masker frequencies (0.75BF, BF, 1.25BF) for 'co-located' and 'far' masker locations, respectively, for both A1 and CM/CL populations. At these masker frequencies, pronounced forward suppression with a magnitude > 20% was observed for both A1 and CM/CL units (Figs 5D and 6D). The PSTHs to the probe alone (at BF) are also shown (gray areas) as a guide to the inspection of the extent of forward suppression.

In A1 (Fig. 8A), the PSTHs to the 'far' masker (dashed lines, 0–100 ms) showed weaker magnitude and longer response latency than those to the 'co-located' masker (black lines, 0–100 ms) at all three frequencies. However, the temporal profiles of PSTHs during the probe period were similar in magnitude and latency between 'far' and 'co-located' maskers (Fig. 8A; 100–200 ms). Figure 8B shows the population PSTHs of CM/CL neurons. Comparing with the A1 population shown in Fig. 8A, the masker responses at the 'far' location were mostly absent. Strikingly, although the on-BF masker presented from the 'far' location evoked no significant excitatory responses, it suppressed the probe responses by an amount similar to the 'co-located' masker (middle plot, Fig. 8B). These data indicate that the strength of forward suppression is not predicted by

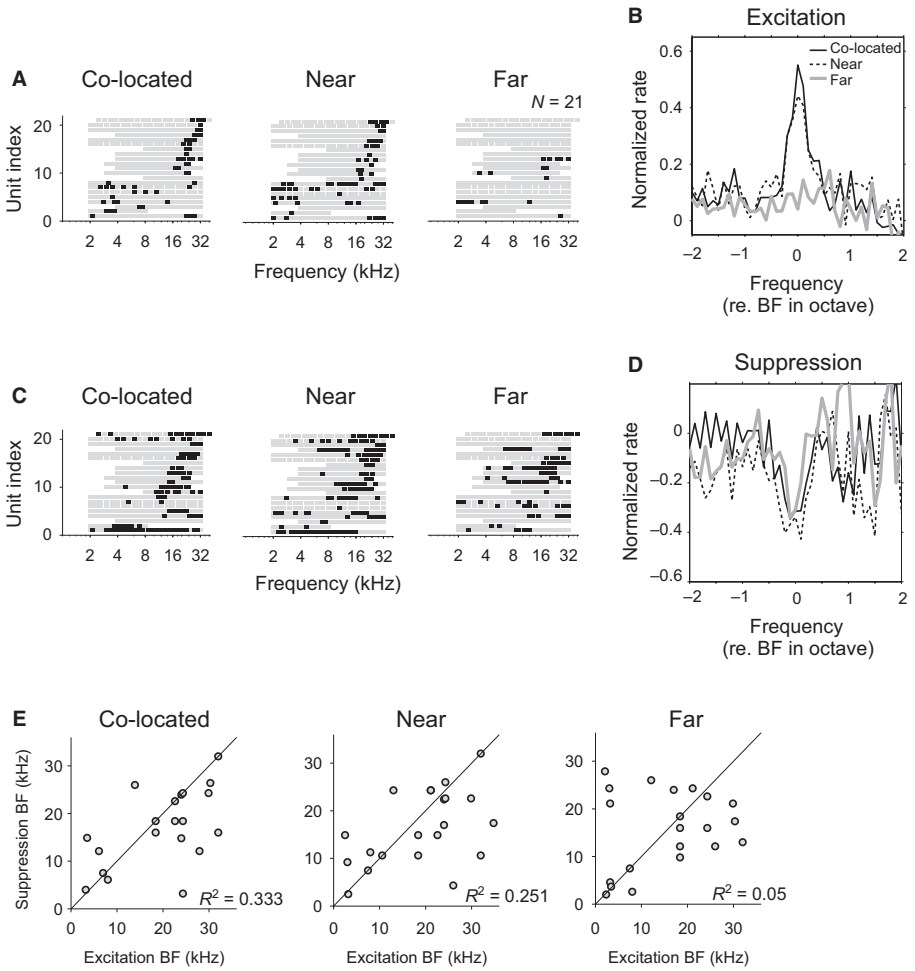

FIG. 6. Population analysis of the spectral extent of forward suppression in CM/CL. Results of CM/CL neurons for tuning of excitation and tuning of forward suppression. The results were presented in the same format as those in Fig. 5. BF, best frequency.

the magnitude of masker responses. We found no significant correlations between changes of masker-evoked responses and changes of suppression at these three masker frequencies (A1: $P > 0.13$; CM/CL: $P > 0.23$; Spearman rank correlation).

On the other hand, if comparisons were made only for results in the 'co-located' condition (black lines) as used in previous research (e.g. Calford & Semple, 1995; Brosch & Schreiner, 1997), on-BF maskers that evoked stronger excitatory responses also caused stronger forward suppression than off-BF maskers. One possible explanation is that the strength of inhibition is stronger around BF, as suggested by intracellular recording studies (Wehr & Zador, 2003; Kaur *et al.*, 2004; Tan *et al.*, 2004). However, extracellular recordings performed in our study cannot distinguish the inhibitory mechanisms from neural adaptation or fatigue, which may occur when the masker and probe were delivered from the same source location.

Discussion

This study investigates the relationship between forward suppression and masker location in responses of A1 and CM/CL neurons in awake marmoset cortex. The results show that properties of forward suppression remain similar when moving the masker location from center to 'far' regions of a neuron's SRF. This spatial constancy applies to the frequency range of forward suppression (Figs 5 and 6), the shape of the masker tuning curve (Fig. 7), and the time course of forward suppression (Fig. 8). These results provide previously unavailable information about the spectral characteristics of forward suppression across masker locations.

Forward suppression with 'far' masker in auditory cortex

The most noticeable finding of this study is the strong forward suppression evoked by a 'far' masker around BF. To our knowledge, this spatial feature of forward suppression, evoked by narrow-band stimuli, has never been reported in previous studies. In our results (Figs 3 and 4), forward suppression persists at specific masker frequencies when the masker was moved away from the probe. Notably, at the 'far' locations, the masker itself did not or only weakly evoked activity in a neuron. This is seen more often in CM/CL than in A1 (Figs 5 and 6).

Previous studies have shown that the strong forward suppression was associated with BF masker stimuli for the 'co-located' condition (e.g. Harris & Dallos, 1979; Delgutte, 1990; Calford & Semple, 1995; Brosch & Schreiner, 1997; Nelson *et al.*, 2009). Our results show that this frequency dependence of forward suppression remains when the masker and probe were delivered from different locations (Figs 5 and 6). The observed disassociation between masking strength and masker responses contrasts early findings in the auditory nerve fibers (Harris & Dallos, 1979), where forward masking increases with the magnitude of masker-driven responses and

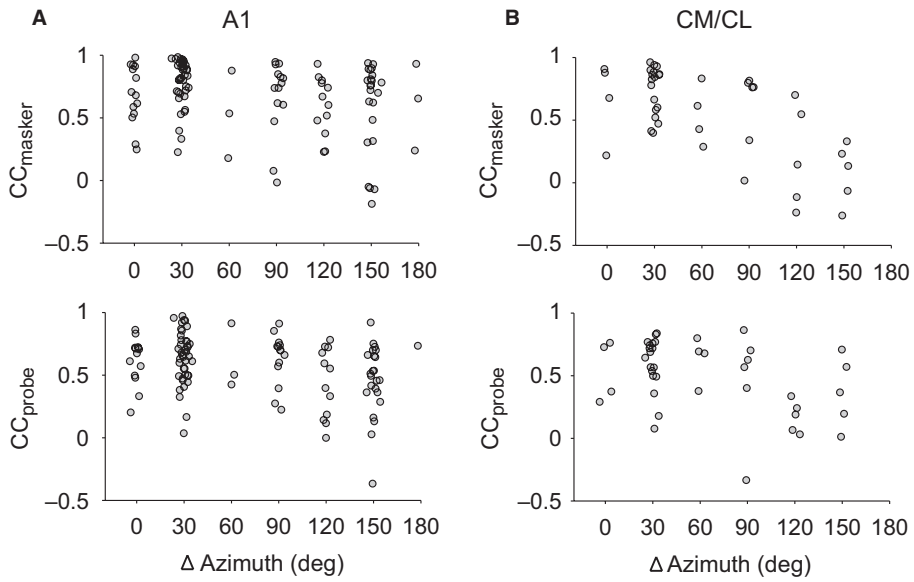

FIG. 7. Changes in the shape of masker tuning function with increasing spatial distance between masker and probe. The relationship between tuning curve similarity and azimuth (AZ) separation between masker and probe in primary auditory cortex (A1; A and B) and caudal medial/caudal lateral (CM/CL; C and D). The data set was based on those presented in Figs 5 and 6. To quantify tuning curve similarity, pair-wise correlations were performed on the results obtained at different masker locations for each neuron. CC_{masker} is the correlation coefficient between a pair of excitatory tuning curves, and CC_{probe} is the correlation coefficient between a pair of inhibitory tuning curves. Data comparing 'co-located' and 'near' conditions had ΔAZ of 0° or 30°, while those comparing 'co-located' and 'far' conditions had ΔAZ > 30°.

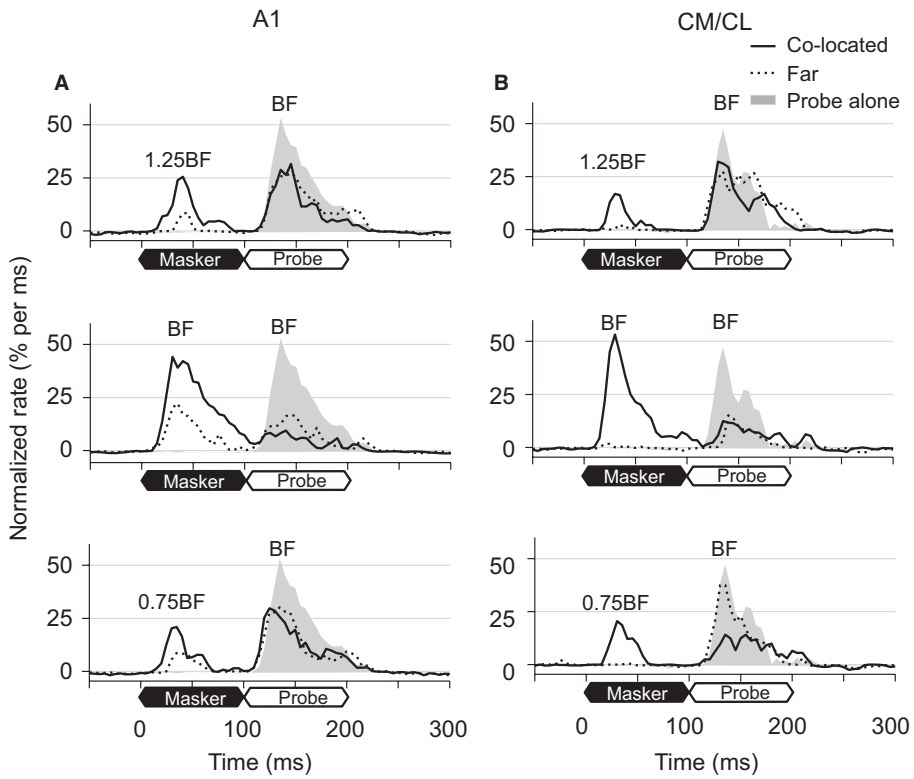

FIG. 8. Effect of masker location on the temporal profile of forward suppression. Population average of PSTHs in response to the masker-probe and to the probe-alone stimuli in primary auditory cortex (A1; A) and caudal medial/caudal lateral (CM/CL; B). For the masker-probe presentation, masker and probe each lasted 100 ms. For the probe-alone presentation, the masker was replaced with 100 ms silence, and the probe [at best frequency (BF)] started at 100 ms. Responses of individual neurons at three masker frequencies (0.75BF, BF, 1.25BF) were extracted and averaged across the population (see Materials and methods for details). Probe-alone responses are shown in gray. The solid and dashed lines on each plot are results for the 'co-located' and 'far' maskers, respectively.

appears to be independent of masker spectral content. In our results, the opposite is seen for 'far' maskers – masking is more effective around BF even though the response to the masker itself is low.

Synaptic inhibition might be one possible mechanism for the observed physiological masking with 'far' maskers. Intracellular research has shown that synaptic inhibition lasts from tens to a few

hundreds of milliseconds in the auditory cortex, depending on the usage of anesthesia (Tan *et al.*, 2004; Wehr & Zador, 2005), and exhibits similar frequency tuning with excitation (Wehr & Zador, 2003). Another possible mechanism is synaptic suppression. One study has shown that the loss of excitatory drive (synaptic suppression) is involved in forward masking beyond 100 ms in response to very brief noise bursts with a 5-ms duration (Wehr & Zador, 2005).

We argue that synaptic suppression is not a primary cause for the observed forward suppression found at the 'far' condition. According to the suppression mechanism, one might predict that compared with those at the 'center' location, the weaker masker responses at the 'far' location would be associated with less spike-driven synaptic fatigue and thus stronger recovery of probe responses. This is not supported by our data, especially not those in CM/CL (Fig. 8). Considering that synaptic inhibition typically outlasts the duration of the stimulus for tens of milliseconds (Wehr & Zador, 2005; Tan *et al.*, 2007) and that the forward suppression we characterized was within the time course of 100 ms after masker offset (Fig. 8), we speculate that the reduction of probe spiking activity found in our study is primarily caused by synaptic inhibition, whose spatial tuning extends broadly in space. Evaluations of this proposal would require a comprehensive examination of synaptic mechanisms underlying the frequency tuning of a neuron at center and far regions of its SRF. This dataset is currently unavailable and the spatial characteristics of synaptic inhibition remain an open question in the auditory cortex. Recently, it has been reported that the spatial tuning of synaptic inhibition is considerably broader than that of synaptic excitation in the visual cortex (V1) of mice in the awake, but not the anesthetized, condition, suggesting that inhibition restrains the spatial extend of neural activity during wakefulness (Haider *et al.*, 2012). At the moment, our knowledge about the synaptic activity in the auditory cortex is exclusively based on intracellular studies of anesthetized animals. It would thus be of great interest to learn, in future research, whether the spatial characteristics of synaptic activity in the auditory cortex also depend on brain state.

A recent study that surveyed, more broadly, the frequency response areas (FRAs) in A1 of anesthetized guinea pig report that in some neurons suppression frequencies align with probe frequency, not BF of a unit (Scholes *et al.*, 2011). Their results suggest that frequency-specific adaptation contributes to observed forward suppression in A1. As reported in previous studies from our laboratory (Sadagopan & Wang, 2008, 2010), the FRAs in A1 of awake marmoset are shaped by inhibitory activities along both frequency and level axes, on which a majority of FRAs (~68%) exhibit 'O'-shaped tuning areas, not 'V'-shaped as shown in Scholes *et al.* (2011). However, few studies have systematically investigated frequency-specific forward masking in the spatial domain, and stimulus-specific adaptation remains an interesting mechanism to be tested on stimuli with distinct spatial locations in future studies.

Implications for neural processing of multiple sound sources

In real-life situations the spatial arrangement between target and masker can vary from moment to moment. Hypothetically, this variability could impede the detectability of a target by single neurons, if their SRFs constrain target or masker information available for neural processing. To the contrary, we found that active sound interactions could occur within and outside the excitatory region of a SRF. In our 'forward-masking' tests, the frequency tuning of forward suppression remains largely unchanged with masker location, showing a primary peak around BF (Figs 5 and 6).

This form of spatial constancy has important implications for understanding the neural functions in encoding multiple sound sources in space. It indicates that cortical neural activity to a driven stimulus (e.g. BF tone at the center location of a SRF) is subject to context modulation. Here the driven activity (probe responses) decreases when a competing stimulus with a similar spectral content is presented at adjacent locations (on-BF masker), and remains unaffected when the competing stimulus has a dissimilar spectral content (off-BF masker). This receptive field property allows change (or contrast) detection across the joint domain of space and frequency by single neurons in the auditory cortex. Similar suppressive surround modulation has been extensively studied in the primary V1 (see Allman *et al.*, 1985; Series *et al.*, 2003 for review), where the maximal surround suppression is mainly caused by stimuli with the same orientation and spatial frequency at center and surround (Knierim & van Essen, 1992; DeAngelis *et al.*, 1994; Li & Li, 1994). The center–surround interaction may serve as a general principle for sensory integration and discrimination in the neocortex.

Untangle spectral and spatial factor in auditory cortex activity

Unlike the visual system, sensory cells at the auditory periphery are not spatially tuned. Spatial selectivity of the auditory system arises from the neural computation of interaural time/level differences and monaural spectral cues at the brainstem (see reviews by Yin, 2002; Young & Davis, 2002), and becomes increasingly complex along the ascending auditory pathway due to convergence of input carrying varying spatial cues (Irvine *et al.*, 1996; McAlpine *et al.*, 1998; Samson *et al.*, 2000; Chase & Young, 2008) and inhibitory modulation (Imig *et al.*, 1997; D'Angelo *et al.*, 2005). As reported by others (Recanzone, 2000; Mickey & Middlebrooks, 2003; Woods *et al.*, 2006; King *et al.*, 2007; Werner-Reiss & Groh, 2008; Lee & Middlebrooks, 2010) and our own study (Zhou & Wang, 2012) using behaving and awake preparations, auditory cortex neurons in A1 and surrounding areas show marked spatial sensitivity with varying tuning width, location selectivity and level tolerance. Nevertheless, few physiological studies have investigated whether non-spatial factors, such as frequency selectivity, change with stimulus location with a few exceptions from auditory midbrain research (Knudsen & Konishi, 1978; Poirier *et al.*, 2003). Notably, these two studies both used a pair of stimuli to probe the frequency tuning of neurons at far regions of SRFs as opposed to the spike-triggered average (STA) method used by others (e.g. Schnupp *et al.*, 2001). This distinction is important because sounds delivered from the far regions of SRFs often do not evoke sufficient spiking activity for STA estimation. Our study also benefits from the two-stimulus approach. We found that long-lasting forward suppression (within 100 ms after masker offset) depends on masker spectral content, but not masker location. This new finding of spatial constancy may help define the complex receptive field properties of cortical neurons in the joint domain of space and frequency.

One unsolved issue in this study is the neural mechanisms underlying the spatial constancy observed. This is not a trivial outcome for the auditory system, in that sounds entering the ears are subject to the directional filtering of the outer ears, as described by the head-related transfer functions (HRTFs; Batteau, 1967). After this filtering, the spectral shape of the ear-canal signal implicitly contains spectral information for sound location (Hebrank & Wright, 1974; Kulkarni & Colburn, 1998) and sound features (such as timbre; Plomp, 1970; Grey, 1977). For the marmoset species, the 12–24 kHz frequency range contains not only the spectral notch information for EL localization (Slee & Young, 2010), but also the second harmonics of mar-

moset vocalization (Epple, 1968; DiMattina & Wang, 2006; Pistorio *et al.*, 2006). In theory, HRTF filtering could generate 'blind spots', at which important vocalization information is compromised.

Early physiological studies have shown that the rate difference profiles among auditory nerve fibers yield discernable correlation with the spectral differences between HRTFs (Poon & Brugge, 1993; Rice *et al.*, 1995). To achieve the observed spatial constancy of frequency tuning in the auditory cortex, the spectral information of sound location (e.g. spectral notches) may be encoded or even resolved by auditory neurons prior to A1 (Young & Davis, 2002; May *et al.*, 2008). Further studies that address both source-related and HRTF-related spectral variability may provide a more detailed description on excitation- and inhibition-based spectral analyses in the auditory cortex.

Comparison of neural response properties between A1 and CM/CL

Based on the population distributions of spatial and spectral tuning widths and monkey call selectivity (Rauschecker *et al.*, 1995; Recanzone, 2000; Tian *et al.*, 2001) and inactivation research (Lomber & Malhotra, 2008), a prevailing view is that the central auditory system is divided into at least two separate streams, the so-called 'what' and 'where' pathways emerging after A1 (Romanski *et al.*, 1999; Kaas & Hackett, 2000). Whether or not the associated neural analyses involve specialized neural groups and/or separate information streams (i.e. 'what' vs. 'where' systems) remains unsettled (Rauschecker *et al.*, 1997; Recanzone & Cohen, 2010). The available evidence indicates that spectro-temporal and spatial information of sound is mixed in A1 (Bizley *et al.*, 2009; Walker *et al.*, 2011). The CM and CL field is one of the subdivisions of the auditory belt area surrounding the auditory core, and is thought to be the initial stage of the 'where' pathway emerging after A1 (Kaas & Hackett, 2000).

In our results, A1 and CM/CL neurons showed marked differences in their BF preference (Fig. 2D) and threshold (Fig. 2E). Note that the caudal area is more compressed in size than A1 (Fig. 2A) because a large portion of CM is located along the lower bank of lateral sulcus (Kajikawa *et al.*, 2005), whereas A1 of marmoset is largely positioned on the surface of the superior temporal gurus. This anatomical difference between A1 and the caudal field makes it easier to obtain the tonotopic mapping in A1 than in CM/CL. Thus, it is possible that the seemingly discontinued frequency representation in CM/CL is influenced by the sampling bias in our measurement.

Comparing with CM/CL, more A1 neurons were tuned to mid-range frequencies (5–10 kHz), consistent with prior work in marmosets (Kajikawa *et al.*, 2005). This frequency range covers the first harmonics of marmoset vocalization (Epple, 1968), and exhibits the lowest thresholds in marmoset audiograms (Seiden, 1957; Osmanski & Wang, 2011). In A1, the threshold curves based on single-unit data we examined using free-field stimulation (Fig. 2F), and obtained by others using close-field stimulation (Aitkin *et al.*, 1986), showed similar trends to the behavioral data. By contrast, the threshold curves did not exhibit clear BF dependence in results of CM/CL neurons (Fig. 2F), indicating further modulations of neural excitability from A1 to CM/CL, as suggested by others (Rauschecker *et al.*, 1997).

On the other hand, the minimum response latency to pure tones was similar or even shorter in CM/CL relative to A1 in marmosets (Kajikawa *et al.*, 2005; fig. 2B in this study) and macaques (Recanzone *et al.*, 2000). This is an intriguing observation in that the caudal field as a secondary cortical field after A1 is expected to show longer latencies, as found in other belt subdivisions (e.g. Recanzone *et al.*, 2000). One explanation is that the caudal field receives direct thalamic input (Morel *et al.*, 1993; Molinari *et al.*, 1995; Rauschecker *et al.*, 1997). In marmosets, projections to CM mostly originate from the anterior dorsal and magnocellular divisions of the medial geniculate complex (MGC), while those to A1 are primarily from the anterior division of the MGC (de la Mothe *et al.*, 2006a,b). The functional specificities of fast thalamic input to the caudal field have not been reported in the literature, especially with regard to their contribution to spatial coding by putative 'where' neurons in CM/CL.

As mentioned above, both A1 and CM/CL neurons showed location-invariant frequency tuning characteristics of forward suppression. This observation suggests that independent modulations of spectral and spatial sound information are preserved in the core-to-caudal-belt pathway. Based on our observation, spatial and spectral processes are not intertwined in a random manner in areas A1 and CM/CL of marmoset auditory cortex.

Acknowledgements

This work was supported by National Institute of Health (grant number DC03180 and DC005808 to X.W.). The authors thank J. Estes and N. Sotuyo for assistance with animal care.

Abbreviations

A1, primary auditory cortex; AZ, azimuth; BF, best frequency; CC, correlation coefficient; CL, caudal lateral; CM, caudal medial; EL, elevation; FRA, frequency response area; HRTF, head-related transfer function; MGC, medial geniculate complex; PSTH, post-stimulus time histogram; SNR, signal-to-noise ratio; SPL, sound pressure level; SRF, spatial receptive field; STA, spike-triggered average; V1, visual cortex.

References

Aitkin, L.M., Merzenich, M.M., Irvine, D.R., Clarey, J.C. & Nelson, J.E. (1986) Frequency representation in auditory cortex of the common marmoset (*Callithrix jacchus jacchus*). *J. Comp. Neurol.*, **252**, 175–185.

Allman, J., Miezin, F. & McGuinness, E. (1985) Stimulus specific responses from beyond the classical receptive field: neurophysiological mechanisms for local-global comparisons in visual neurons. *Annu. Rev. Neurosci.*, **8**, 407–430.

Batteau, D.W. (1967) The role of the pinna in human localization. *P. Roy. Soc. Lond. B Bio.*, **168**, 158–180.

Bendor, D. & Wang, X. (2008) Neural response properties of primary, rostral, and rostrotemporal core fields in the auditory cortex of marmoset monkeys. *J. Neurophysiol.*, **100**, 888–906.

Bizley, J.K., Walker, K.M., Silverman, B.W., King, A.J. & Schnupp, J.W. (2009) Interdependent encoding of pitch, timbre, and spatial location in auditory cortex. *J. Neurosci.*, **29**, 2064–2075.

Brosch, M. & Schreiner, C.E. (1997) Time course of forward masking tuning curves in cat primary auditory cortex. *J. Neurophysiol.*, **77**, 923–943.

Calford, M.B. & Semple, M.N. (1995) Monaural inhibition in cat auditory cortex. *J. Neurophysiol.*, **73**, 1876–1891.

Chase, S.M. & Young, E.D. (2008) Cues for sound localization are encoded in multiple aspects of spike trains in the inferior colliculus. *J. Neurophysiol.*, **99**, 1672–1682.

Dahmen, J.C., Keating, P., Nodal, F.R., Schulz, A.L. & King, A.J. (2010) Adaptation to stimulus statistics in the perception and neural representation of auditory space. *Neuron*, **66**, 937–948.

D'Angelo, W.R., Sterbing, S.J., Ostapoff, E.M. & Kuwada, S. (2005) Role of GABAergic inhibition in the coding of interaural time differences of low-frequency sounds in the inferior colliculus. *J. Neurophysiol.*, **93**, 3390–3400.

DeAngelis, G.C., Freeman, R.D. & Ohzawa, I. (1994) Length and width tuning of neurons in the cat's primary visual cortex. *J. Neurophysiol.*, **71**, 347–374.

Delgutte, B. (1990) Physiological mechanisms of psychophysical masking: observations from auditory-nerve fibers. *J. Acoust. Soc. Am.*, **87**, 791–809.

DiMattina, C. & Wang, X. (2006) Virtual vocalization stimuli for investigating neural representations of species-specific vocalizations. *J. Neurophysiol.*, **95**, 1244–1262.

Epple, G. (1968) Comparative studies on vocalization in marmoset monkeys (Hapalidae). *Folia Primatol. (Basel)*, **8**, 1–40.

Fitzpatrick, D.C., Kuwada, S., Kim, D.O., Parham, K. & Batra, R. (1999) Responses of neurons to click-pairs as simulated echoes: auditory nerve to auditory cortex. *J. Acoust. Soc. Am.*, **106**, 3460–3472.
Fletcher, H. (1940) Auditory patterns. *Rev. Mod. Phys.*, **12**, 47–65.
Grey, J.M. (1977) Multidimensional perceptual scaling of musical timbres. *J. Acoust. Soc. Am.*, **61**, 1270–1277.
Haider, B., Hausser, M. & Carandini, M. (2012) Inhibition dominates sensory responses in the awake cortex. *Nature*, **493**, 97–100.
Harris, D.M. & Dallos, P. (1979) Forward masking of auditory nerve fiber responses. *J. Neurophysiol.*, **42**, 1083–1107.
Hebrank, J. & Wright, D. (1974) Spectral cues used in the localization of sound sources on the median plane. *J. Acoust. Soc. Am.*, **56**, 1829–1834.
Imig, T.J., Poirier, P., Irons, W.A. & Samson, F.K. (1997) Monaural spectral contrast mechanism for neural sensitivity to sound direction in the medial geniculate body of the cat. *J. Neurophysiol.*, **78**, 2754–2771.
Irvine, D.R., Rajan, R. & Aitkin, L.M. (1996) Sensitivity to interaural intensity differences of neurons in primary auditory cortex of the cat. I. types of sensitivity and effects of variations in sound pressure level. *J. Neurophysiol.*, **75**, 75–96.
Kaas, J.H. & Hackett, T.A. (2000) Subdivisions of auditory cortex and processing streams in primates. *Proc. Natl. Acad. Sci. USA*, **97**, 11793–11799.
Kajikawa, Y., de La Mothe, L., Blumell, S. & Hackett, T.A. (2005) A comparison of neuron response properties in areas A1 and CM of the marmoset monkey auditory cortex: tones and broadband noise. *J. Neurophysiol.*, **93**, 22–34.
Kaur, S., Lazar, R. & Metherate, R. (2004) Intracortical pathways determine breadth of subthreshold frequency receptive fields in primary auditory cortex. *J. Neurophysiol.*, **91**, 2551–2567.
King, A.J., Bajo, V.M., Bizley, J.K., Campbell, R.A., Nodal, F.R., Schulz, A.L. & Schnupp, J.W. (2007) Physiological and behavioral studies of spatial coding in the auditory cortex. *Hearing Res.*, **229**, 106–115.
Knierim, J.J. & van Essen, D.C. (1992) Neuronal responses to static texture patterns in area V1 of the alert macaque monkey. *J. Neurophysiol.*, **67**, 961–980.
Knudsen, E.I. & Konishi, M. (1978) Space and frequency are represented separately in auditory midbrain of the owl. *J. Neurophysiol.*, **41**, 870–884.
Kulkarni, A. & Colburn, H.S. (1998) Role of spectral detail in sound-source localization. *Nature*, **396**, 747–749.
Lane, C.C. & Delgutte, B. (2005) Neural correlates and mechanisms of spatial release from masking: single-unit and population responses in the inferior colliculus. *J. Neurophysiol.*, **94**, 1180–1198.
Lee, C.C. & Middlebrooks, J.C. (2010) Auditory cortex spatial sensitivity sharpens during task performance. *Nat. Neurosci.*, **14**, 108–114.
Li, C.Y. & Li, W. (1994) Extensive integration field beyond the classical receptive field of cat's striate cortical neurons–classification and tuning properties. *Vision Res.*, **34**, 2337–2355.
Litovsky, R.Y. & Yin, T.C. (1998) Physiological studies of the precedence effect in the inferior colliculus of the cat. II. Neural mechanisms. *J. Neurophysiol.*, **80**, 1302–1316.
Lomber, S.G. & Malhotra, S. (2008) Double dissociation of 'what' and 'where' processing in auditory cortex. *Nat. Neurosci.*, **11**, 609–616.
Lu, T., Liang, L. & Wang, X. (2001) Neural representations of temporally asymmetric stimuli in the auditory cortex of awake primates. *J. Neurophysiol.*, **85**, 2364–2380.
May, B.J., Anderson, M. & Roos, M. (2008) The role of broadband inhibition in the rate representation of spectral cues for sound localization in the inferior colliculus. *Hearing Res.*, **238**, 77–93.
McAlpine, D., Jiang, D., Shackleton, T.M. & Palmer, A.R. (1998) Convergent input from brainstem coincidence detectors onto delay-sensitive neurons in the inferior colliculus. *J. Neurosci.*, **18**, 6026–6039.
Merzenich, M.M. & Brugge, J.F. (1973) Representation of the cochlear partition of the superior temporal plane of the macaque monkey. *Brain Res.*, **50**, 275–296.
Mickey, B.J. & Middlebrooks, J.C. (2003) Representation of auditory space by cortical neurons in awake cats. *J. Neurosci.*, **23**, 8649–8663.
Mickey, B.J. & Middlebrooks, J.C. (2005) Sensitivity of auditory cortical neurons to the locations of leading and lagging sounds. *J. Neurophysiol.*, **94**, 979–989.
Middlebrooks, J.C. & Bremen, P. (2013) Spatial stream segregation by auditory cortical neurons. *J. Neurosci.*, **33**, 10986–11001.
Middlebrooks, J.C. & Pettigrew, J.D. (1981) Functional classes of neurons in primary auditory cortex of the cat distinguished by sensitivity to sound location. *J. Neurosci.*, **1**, 107–120.
Molinari, M., Dell'Anna, M.E., Rausell, E., Leggio, M.G., Hashikawa, T. & Jones, E.G. (1995) Auditory thalamocortical pathways defined in monkeys by calcium-binding protein immunoreactivity. *J. Comp. Neurol.*, **362**, 171–194.
Morel, A., Garraghty, P.E. & Kaas, J.H. (1993) Tonotopic organization, architectonic fields, and connections of auditory cortex in macaque monkeys. *J. Comp. Neurol.*, **335**, 437–459.
de la Mothe, L.A., Blumell, S., Kajikawa, Y. & Hackett, T.A. (2006a) Cortical connections of the auditory cortex in marmoset monkeys: core and medial belt regions. *J. Comp. Neurol.*, **496**, 27–71.
de la Mothe, L.A., Blumell, S., Kajikawa, Y. & Hackett, T.A. (2006b) Thalamic connections of the auditory cortex in marmoset monkeys: core and medial belt regions. *J. Comp. Neurol.*, **496**, 72–96.
Nelson, P.C., Smith, Z.M. & Young, E.D. (2009) Wide-dynamic-range forward suppression in marmoset inferior colliculus neurons is generated centrally and accounts for perceptual masking. *J. Neurosci.*, **29**, 2553–2562.
Osmanski, M.S. & Wang, X. (2011) Measurement of absolute auditory thresholds in the common marmoset (*Callithrix jacchus*). *Hearing Res.*, **277**, 127–133.
Oxenham, A.J. (2001) Forward masking: adaptation or integration? *J. Acoust. Soc. Am.*, **109**, 732–741.
Park, T.J., Brand, A., Koch, U., Ikebuchi, M. & Grothe, B. (2008) Dynamic changes in level influence spatial coding in the lateral superior olive. *Hearing Res.*, **238**, 58–67.
Pistorio, A.L., Vintch, B. & Wang, X. (2006) Acoustic analysis of vocal development in a New World primate, the common marmoset (*Callithrix jacchus*). *J. Acoust. Soc. Am.*, **120**, 1655–1670.
Plomp, R. (1964) Rate of decay of auditory sensation. *J. Acoust. Soc. Am.*, **36**, 277–282.
Plomp, R. (1970) Imbre as a multidimensional attribute of complex tones. In Plomp, R. & Smoorenburg, G.F. (Eds), *Frequency Analysis and Periodicity Detection in Hearing*. Sijthoff, Leiden, pp. 397–414.
Poirier, P., Samson, F.K. & Imig, T.J. (2003) Spectral shape sensitivity contributes to the azimuth tuning of neurons in the cat's inferior colliculus. *J. Neurophysiol.*, **89**, 2760–2777.
Poon, P.W. & Brugge, J.F. (1993) Sensitivity of auditory nerve fibers to spectral notches. *J. Neurophysiol.*, **70**, 655–666.
Rauschecker, J.P., Tian, B. & Hauser, M. (1995) Processing of complex sounds in the macaque nonprimary auditory cortex. *Science*, **268**, 111–114.
Rauschecker, J.P., Tian, B., Pons, T. & Mishkin, M. (1997) Serial and parallel processing in rhesus monkey auditory cortex. *J. Comp. Neurol.*, **382**, 89–103.
Reale, R.A. & Brugge, J.F. (2000) Directional sensitivity of neurons in the primary auditory (AI) cortex of the cat to successive sounds ordered in time and space. *J. Neurophysiol.*, **84**, 435–450.
Recanzone, G.H. (2000) Spatial processing in the auditory cortex of the macaque monkey. *Proc. Natl. Acad. Sci. USA*, **97**, 11829–11835.
Recanzone, G.H. & Cohen, Y.E. (2010) Serial and parallel processing in the primate auditory cortex revisited. *Behav. Brain Res.*, **206**, 1–7.
Recanzone, G.H., Guard, D.C. & Phan, M.L. (2000) Frequency and intensity response properties of single neurons in the auditory cortex of the behaving macaque monkey. *J. Neurophysiol.*, **83**, 2315–2331.
Rice, J.J., Young, E.D. & Spirou, G.A. (1995) Auditory-nerve encoding of pinna-based spectral cues: rate representation of high-frequency stimuli. *J. Acoust. Soc. Am.*, **97**, 1764–1776.
Romanski, L.M., Tian, B., Fritz, J., Mishkin, M., Goldman-Rakic, P.S. & Rauschecker, J.P. (1999) Dual streams of auditory afferents target multiple domains in the primate prefrontal cortex. *Nat. Neurosci.*, **2**, 1131–1136.
Sachs, M.B. & Kiang, N.Y. (1968) Two-tone inhibition in auditory-nerve fibers. *J. Acoust. Soc. Am.*, **43**, 1120–1128.
Sadagopan, S. & Wang, X. (2008) Level invariant representation of sounds by populations of neurons in primary auditory cortex. *J. Neurosci.*, **28**, 3415–3426.
Sadagopan, S. & Wang, X. (2010) Contribution of inhibition to stimulus selectivity in primary auditory cortex of awake primates. *J. Neurosci.*, **30**, 7314–7325.
Samson, F.K., Barone, P., Irons, W.A., Clarey, J.C., Poirier, P. & Imig, T.J. (2000) Directionality derived from differential sensitivity to monaural and binaural cues in the cat's medial geniculate body. *J. Neurophysiol.*, **84**, 1330–1345.
Schnupp, J.W., Mrsic-Flogel, T.D. & King, A.J. (2001) Linear processing of spatial cues in primary auditory cortex. *Nature*, **414**, 200–204.
Scholes, C., Palmer, A.R. & Sumner, C.J. (2011) Forward suppression in the auditory cortex is frequency-specific. *Eur. J. Neurosci.*, **33**, 1240–1251.

Seiden, H.R. (1957) Auditory acuity of the marmoset monkey (Hapale jacchus). PhD Thesis. Princeton University, Princeton, NJ.
Series, P., Lorenceau, J. & Fregnac, Y. (2003) The "silent" surround of V1 receptive fields: theory and experiments. *J. Physiol. Paris*, **97**, 453–474.
Slee, S.J. & Young, E.D. (2010) Sound localization cues in the marmoset monkey. *Hearing Res.*, **260**, 96–108.
Sutter, M.L., Schreiner, C.E., McLean, M., O'Connor, K.N. & Loftus, W.C. (1999) Organization of inhibitory frequency receptive fields in cat primary auditory cortex. *J. Neurophysiol.*, **82**, 2358–2371.
Tan, A.Y., Zhang, L.I., Merzenich, M.M. & Schreiner, C.E. (2004) Tone-evoked excitatory and inhibitory synaptic conductances of primary auditory cortex neurons. *J. Neurophysiol.*, **92**, 630–643.
Tan, A.Y., Atencio, C.A., Polley, D.B., Merzenich, M.M. & Schreiner, C.E. (2007) Unbalanced synaptic inhibition can create intensity-tuned auditory cortex neurons. *Neuroscience*, **146**, 449–462.
Tian, B., Reser, D., Durham, A., Kustov, A. & Rauschecker, J.P. (2001) Functional specialization in rhesus monkey auditory cortex. *Science*, **292**, 290–293.
Walker, K.M., Bizley, J.K., King, A.J. & Schnupp, J.W. (2011) Multiplexed and robust representations of sound features in auditory cortex. *J. Neurosci.*, **31**, 14565–14576.
Wehr, M. & Zador, A.M. (2003) Balanced inhibition underlies tuning and sharpens spike timing in auditory cortex. *Nature*, **426**, 442–446.
Wehr, M. & Zador, A.M. (2005) Synaptic mechanisms of forward suppression in rat auditory cortex. *Neuron*, **47**, 437–445.
Werner-Reiss, U. & Groh, J.M. (2008) A rate code for sound azimuth in monkey auditory cortex: implications for human neuroimaging studies. *J. Neurosci.*, **28**, 3747–3758.
Woods, T.M., Lopez, S.E., Long, J.H., Rahman, J.E. & Recanzone, G.H. (2006) Effects of stimulus azimuth and intensity on the single-neuron activity in the auditory cortex of the alert macaque monkey. *J. Neurophysiol.*, **96**, 3323–3337.
Yin, T.C. (2002) Neural mechanisms of encoding binaural localization cues in the auditory brainstem. In Oertel, D., Fay, R.R. & Popper, A.N. (Eds), *Integrative Functions in the Mammalian Auditory Brainstem*. Springer-Verlag, New York, pp. 99–159.
Young, E.D. & Davis, K.A. (2002) Circuitry and Function of the Dorsal Cochlear Nucleus. In Oertel, D., Popper, A.N. & Fay, R.R. (Eds), *Integrative Functions in the Mammalian Auditory Pathway*. Springer-Verlag, New York, pp. 160–206.
Zhou, Y. & Wang, X. (2012) Level dependence of spatial processing in the primate auditory cortex. *J. Neurophysiol.*, **108**, 810–826.
Zhou, B., Green, D.M. & Middlebrooks, J.C. (1992) Characterization of external ear impulse responses using Golay codes. *J. Acoust. Soc. Am.*, **92**, 1169–1171.